AFRL-AFOSR-JP-TR-2017-0071

Core-Shell Photonic Nanoparticles for Enhanced Solar-to-Fuel Photocatalytic Conversion

Randall Lee
UNIVERSITY OF HOUSTON SYSTEM

10/11/2017
Final Report

Air Force Research Laboratory
AF Office Of Scientific Research (AFOSR)/ IOA
Arlington, Virginia 22203
Air Force Materiel Command

REPORT DOCUMENTATION PAGE

Form Approved
OMB No. 0704-0188

1. REPORT DATE *(DD-MM-YYYY)*	2. REPORT TYPE	3. DATES COVERED *(From - To)*
16-10-2017	Final	12 Jul 2016 to 11 Oct 2017

4. TITLE AND SUBTITLE
Core-Shell Photonic Nanoparticles for Enhanced Solar-to-Fuel Photocatalytic Conversion

5a. CONTRACT NUMBER

5b. GRANT NUMBER
FA2386-16-1-4067

5c. PROGRAM ELEMENT NUMBER
61102F

6. AUTHOR(S)
Randall Lee

5d. PROJECT NUMBER

5e. TASK NUMBER

5f. WORK UNIT NUMBER

7. PERFORMING ORGANIZATION NAME(S) AND ADDRESS(ES)
UNIVERSITY OF HOUSTON SYSTEM
4800 CALHOUN ST STE 316
HOUSTON, TX 77204-0001 US

8. PERFORMING ORGANIZATION REPORT NUMBER

9. SPONSORING/MONITORING AGENCY NAME(S) AND ADDRESS(ES)
AOARD
UNIT 45002
APO AP 96338-5002

10. SPONSOR/MONITOR'S ACRONYM(S)
AFRL/AFOSR IOA

11. SPONSOR/MONITOR'S REPORT NUMBER(S)
AFRL-AFOSR-JP-TR-2017-0071

12. DISTRIBUTION/AVAILABILITY STATEMENT
A DISTRIBUTION UNLIMITED: PB Public Release

13. SUPPLEMENTARY NOTES

14. ABSTRACT
Professors Randall Lee of UH and Tai-Chou Lee of NCU, Taiwan have been successful at their planned research for this research grant in bimetallic nanoshells that enhance the photocatalytic activity of semiconducting materials. They synthesized and functionalized titanium dioxide nanoparticles with a partial shell of gold. Their research also characterized the photocatalytic activity. The second area was the tuning the dielectric environment of the nanoparticles with think layers of silica and tin oxide. The newly synthesized materials pave the way to the optimization of solar hydrogen production.

The collaborative project has led to 5 peer reviewed publications in several peer reviewed publications, with 9 combined invited talks and poster sessions of their research. During this time the professors also initiated discussions and collaborations with AFRL and industry.

15. SUBJECT TERMS
Metal Nanoshells, Solar Energy Conversion, Photocatalysis, Photochemistry, Dielectric Tuning, Nanoparticle Arrays, Photonic Coupling

16. SECURITY CLASSIFICATION OF:			17. LIMITATION OF ABSTRACT	18. NUMBER OF PAGES	19a. NAME OF RESPONSIBLE PERSON
a. REPORT	b. ABSTRACT	c. THIS PAGE			CHEN, JERMONT
Unclassified	Unclassified	Unclassified	SAR	13	19b. TELEPHONE NUMBER *(Include area code)* 315-227-7007

Professor T. Randall Lee
University of Houston

Professor Tai-Chou Lee
National Central University

Final Report for AOARD Grant FA2386-16-1-4067 "Core-Shell Photonic Nanoparticles and Self-Assembled Arrays for Enhancing Solar-to-Fuel Photocatalytic Conversion"

Date: October 11, 2017

PI and Co-PI information:
PI: T. Randall Lee, trlee@uh.edu; University of Houston; Department of Chemistry; 4800 Calhoun Road, Houston, Texas 77204, United States; +1-713-743-2724

Co-PI: Tai-Chou Lee; taichoulee@ncu.edu.tw; National Central University; Department of Chemical and Materials Engineering; 300 Jhongda Road, Jhongli District, Taoyuan County, Taiwan; +886-3-4227151#34211

Period of Performance: July/12/2016 – July/11/2017

Abstract

Research funded by this award focused on expanding our successful investigation of bimetallic nanoshells that enhance the photocatalytic activity of semiconducting materials. Our earlier work focused on the synthesis of plasmonic gold-silver nanoshells (GS-NSs) having tunable localized surface plasmon resonances (LSPRs) and coated with an outer silica shell. When coupled with a zinc indium sulfide ($ZnIn_2S_4$; ZIS) photocatalyst, the GS-NSs led to the enhancement of hydrogen production of by a factor of 2.6 times compared to the photocatalyst without the plasmonic GS-NSs. The development of these plasmonic/semiconductor composites showed that both the extinction maximum of the GS-NSs as well as the thickness of the outer silica shell have a direct effect on the lifetime of photo-generated electrons in the conduction band of the ZIS photocatalyst. Thus, we focused our recent research efforts on three main thrusts. The first includes the synthesis and application of titanium dioxide nanoparticles coated with a partial gold shell as an alternative photocatalyst. In this aspect, we synthesized anatase TiO_2 nanoparticles ($ATiO_2$) and subsequently functionalized them with a partial gold shell in efforts to broaden their optical extinction into the visible region. Furthermore, coating the $ATiO_2$ particles with a gold shell also suppresses the radiative electron-hole recombination processes that occur in the semiconductor matrix. These features gave rise to an enhanced rate of hydrogen production using $ATiO_2$-AuNS nanoparticles as photocatalysts in the water-splitting reaction. The second thrust focused on tuning the dielectric environment of GS-NS nanoparticles by coating them with thin layers (or "shells") of silica or tin oxide. Preliminary studies also sought to coat the GS-NSs with zinc- and antimony-doped SnO_2, a method that should allow modulating the band gap of the semiconducting material. Additionally, we explored the synthesis and optical properties of photonic iron oxide as a co-catalyst in the photocatalytic splitting of water. These newly synthesized materials pave the way to the optimization of solar hydrogen production via nanoscale engineering.

Introduction

The research described herein focuses on the development of novel optically responsive nanoparticles aimed at enhancing the photocatalytic properties of semiconducting materials in solar-to-fuel catalytic conversion. Depending on the morphology of the type of metal nanoparticles, the corresponding response to light can range from the ultra-violet (UV) to the near infrared (NIR) regions of the electromagnetic spectrum due to changes in the localized surface plasmon resonance (LSPR) associated with the targeted nanoparticles. Our recently published work on the incorporation of gold-silver nanoshells (GS-NS) within a semiconducting matrix composed of zinc indium sulfide ($ZnIn_2S_4$; ZIS) led to an expansion of the activity of the photocatalyst into the visible region. Additionally, depending on the thickness of the silica interlayer, the rate of hydrogen production increased up to 2.6 times that of undoped ZIS. Therefore, developing new and improved types of optically-responsive nanocomposites composed of nanoparticles/semiconductors will provide better solar-to-fuel conversion systems that can ultimately be used as energy-generating structures in remote locations.

Motivated by the results of our GS-NS@SiO_2@ZIS photocatalyst system, we chose to advance our research by pursuing three separate avenues. The first focuses on developing photocatalytic systems that are easily prepared and economically attractive; specifically, the development of titanium dioxide (TiO_2) nanoparticles coated with a partial gold shell as a discrete photocatalyst. The second class of nanoparticles that we developed under this grant aimed at tuning the dielectric layer surrounding the GS-NS nanoparticles using thin silica shells. We also explored the synthesis of plasmonic nanoparticles coated with tin oxide and doped tin oxide. In a third set of studies, we explored the synthesis of photonic iron oxide nanoparticles to serve as co-catalysts in the water-splitting reaction for solar-to-hydrogen photocatalytic conversion.

Results and Discussion

1. Anatase-TiO_2 nanoparticles coated with partial gold shells as alternative photocatalysts

In our search to develop alternative photocatalytic materials that are easily prepared and economically attractive, our group has been exploring the study and use of titanium dioxide (TiO_2) nanoparticles that are decorated with partial gold shells to serve as photocatalysts in a variety of applications. Importantly, unmodified TiO_2 is a low-cost material that is used in applications such as water splitting for hydrogen production, light capture for solar cells, organic material degradation for water and soil remediation, and a variety of antibacterial applications.[1,2] As nanomaterials, the efficiency of the photocatalytic activity of TiO_2 NPs depends on their size, morphology, crystalline phase, surface chemical state, dispersibility in solution, and synthesis procedure. Thus, we prepared custom-designed anatase TiO_2 nanoparticles having an average diameter of ~200 nm by converting their amorphous precursor particles using hydrothermal[3] ($ATiO_2$) or hydrogenation ($HTiO_2$) treatments in efforts to maximize their photocatalytic activity. Yet, the photocatalytic activity of this class of materials suffers from the narrow range of extinctions near the UV region. Therefore, we coated the as-synthesized anatase TiO_2 NPs with a partial Au shell, which broadened their optical absorbance/scattering into the visible region (~650 nm) following the recipe highlighted below in *Scheme 1*.

Scheme 1. Strategy Used for the Preparation of $ATiO_2$-Au Nanoshells ($ATiO_2$-AuNSs)

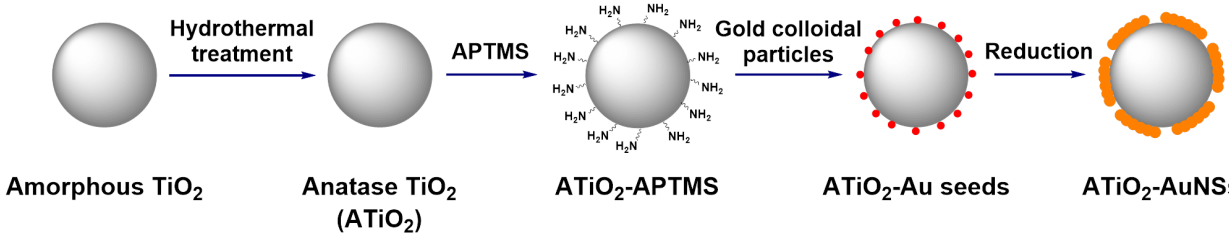

Figure 1 shows the SEM and TEM images of the synthesized TiO_2-AuNSs. Importantly, the X-ray diffraction (XRD) pattern in Figure 1c shows that anatase peaks from the samples are still observed even after deposition of the Au shell. Specifically, the peak at 25.3º is consistent with an anatase phase. Upon deposition of the Au shells, the intensity of the anatase peaks was reduced without influencing the crystal structure of the TiO_2 nanoparticles.

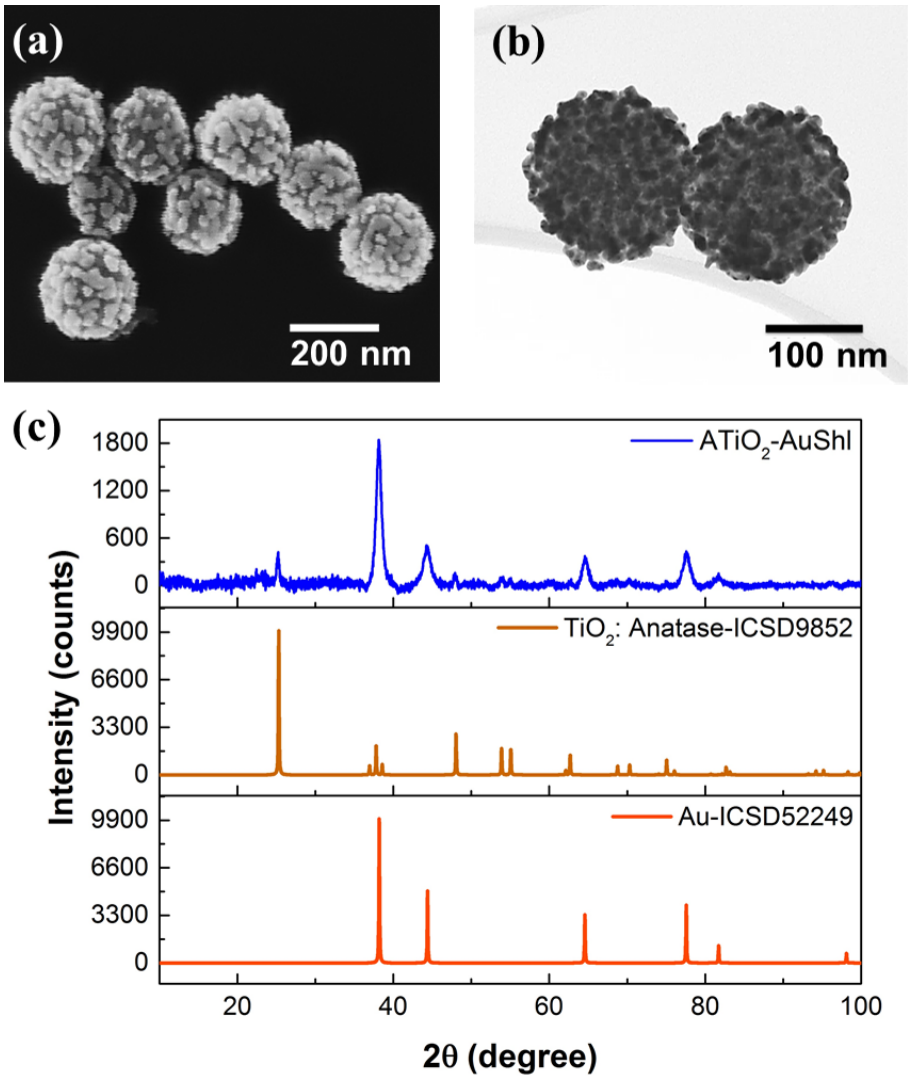

Figure 1. $ATiO_2$-AuNSs (a) SEM, (b) TEM, and (c) XRD patterns of the $ATiO_2$-AuNSs nanoparticles compared to the standard database.

To pursue a systematic study, we supplied our collaborator, Tai-Chou Lee (TCL), with three separate samples: (1) TiO_2 NPs, (2) TiO_2 NPs decorated with 1-5 nm colloidal gold NPs (TiO_2-Au seeding), and (3) TiO_2 NPs coated with a partial gold shell (TiO_2-AuNSs). The TCL group evaluated the photocatalytic production of H_2 for the three types of particles under irradiation by a xenon lamp (a light source used to simulate solar light). The TiO_2-AuNSs exhibited enhanced hydrogen production, as shown in Figure 2, when compared to the other two samples. The results of these studies, which have been submitted for publication as an Article in the *Journal of Colloid and Interface Science*,[4] indicate that the morphology of the gold grown on the TiO_2 NPs has a direct effect on the optical activity and a subsequent increase in the photocatalytic activity of the corresponding TiO_2 particles (i.e., plasmonic enhancement).

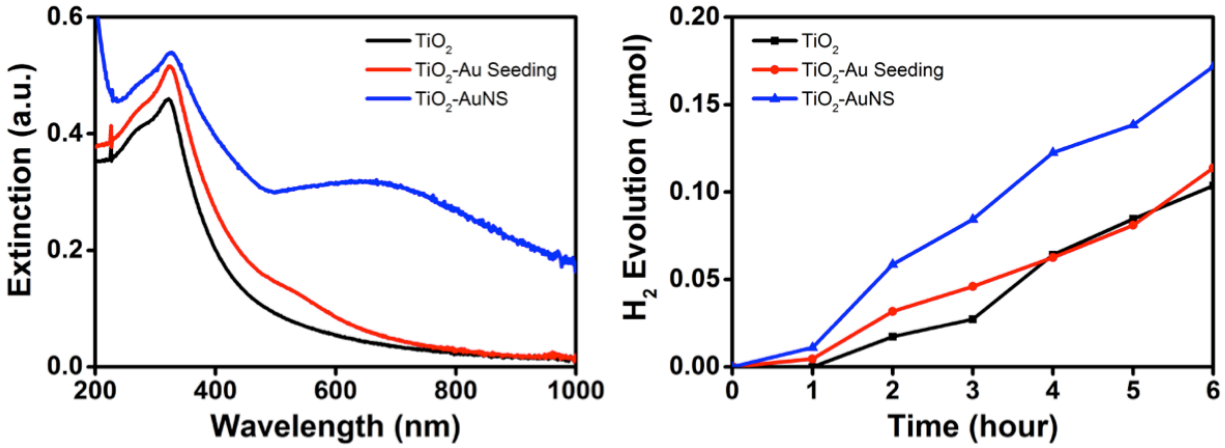

Figure 2. Extinction spectra for the TiO_2, TiO_2-Au Seeding, and TiO_2-AuNS particles (Left). H_2 evolution upon exposure to a xenon lamp as a function of reaction time for the TiO_2, TiO_2-Au Seeding, and TiO_2-AuNS particles (Right).

2. Tuning the dielectric environment surrounding the GS-NS nanostructures

SiO_2–Coated GS-NS Composites. Our recent study has shown that the incorporation of a silica interlayer in the GS-NS/ZIS composite photocatalyst led to a 2.6-fold enhancement in the rate of H_2 production.[5] Moreover, time-resolved photoluminescence data showed that the most effective separation of the electron-hole pairs occurred when the thickness of the SiO_2 interlayer between the ZIS and the GS-NS core was the thinnest (~17 nm), which corresponded to the GS-NS@SiO2@ZIS photocatalyst system that gave the maximum production of H_2.[5] Therefore, we pursued the synthesis of hollow GS-NS nanoparticles that are coated with a thinner silica shell interlayer (~15 nm, ~10 nm, ~5 nm, and ~2 nm). Silica-coated hollow gold-silver nanoshell particles were successfully synthesized in 3 steps. Our initial step included the preparation of silver nanoparticles (AgNPs) by modifying the KI-assisted ascorbic acid/citrate reduction protocol. This step was followed by the synthesis of hollow GS-NS particles via galvanic replacement, as shown in *Scheme 2*. Varying the ratio of the AgNPs to Au salt solution allowed for tuning the extinction maxima associated with the LSPR peaks of the GS-NSs from the visible to NIR. Additionally, controlling the concentrations of (3-aminopropyl)trimethoxysilane (APTMS) and sodium silicate in the reaction mixture afforded silica shell coatings on the GS-NS nanoparticles having tunable thicknesses.

Scheme 2. Strategy for the Preparation of GS-NS Nanoparticles Coated with Thin Silica Shells.

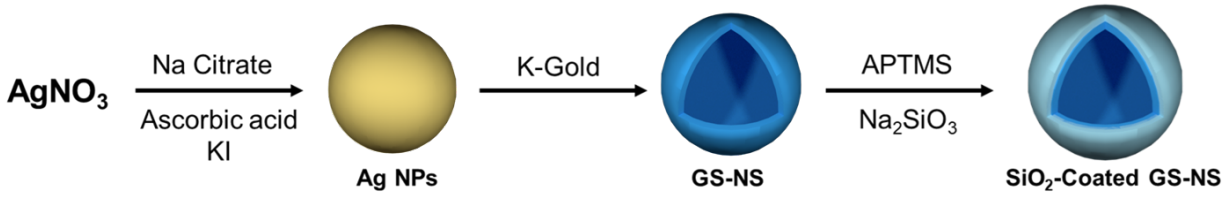

Analysis by SEM and TEM confirmed the size and morphology of the as-prepared nanoparticles (see Figures 3 and 4). Figure 3 shows that the size of the AgNPs and GS-NSs ranged from 60–80 nm. Additionally, increasing the K-gold solution ratio led to a decrease in the thickness of the GS-NSs. Separately, the TEM images in Figure 4 confirmed the three different thicknesses of the silica shells (~2 nm, 10 nm, and 15 nm).

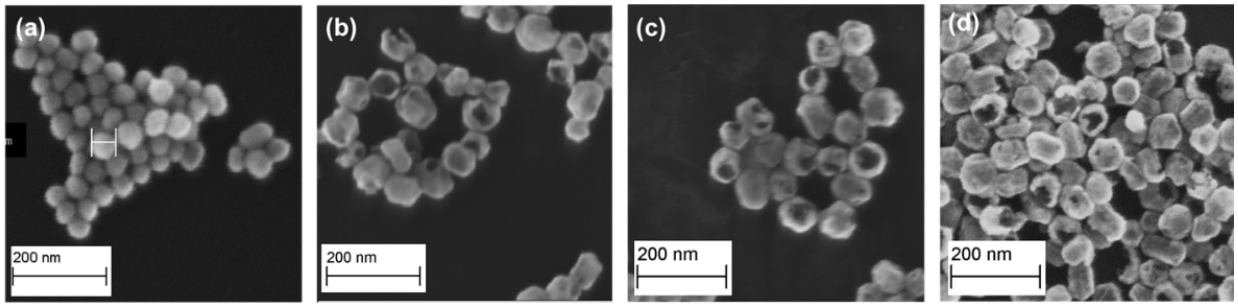

Figure 3. SEM images of (a) silver nanoparticles and the GS-NSs synthesized with (b) 12.5 mL, (c) 30 mL, (d) and 150 mL of K-gold solution.

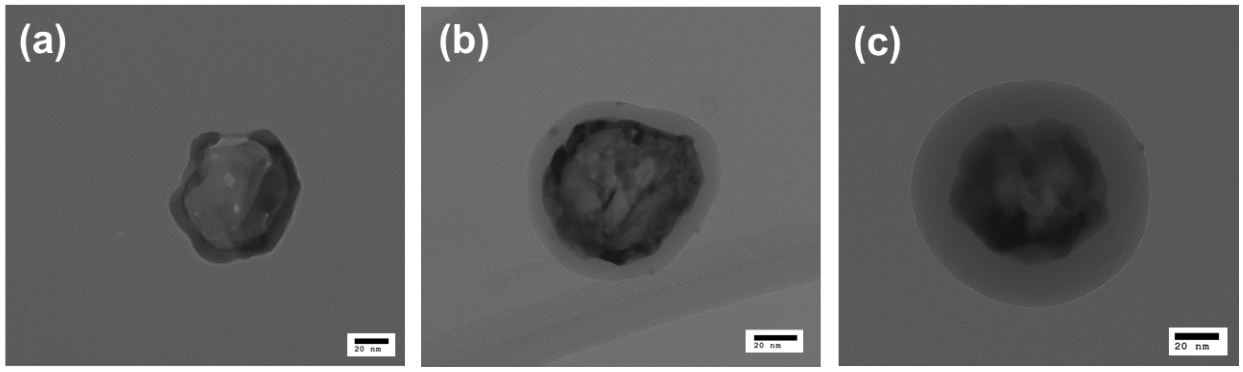

Figure 4. TEM images of hollow GS-NS nanoparticles coated with thin silica shells. The thicknesses of the silica shells were: (a) ~2 nm, (b) ~10 nm, and (c) ~15 nm.

Figure 5 shows that the extinction spectra of the GS-NSs with different shell thicknesses have tunable LSPR peaks at ~500 nm, 700 nm, and 900 nm. The subsequent coating of the GS-NS nanoparticles with silica shells gave rise to only a slight red shift in the corresponding LSPR peaks. Moreover, for a set of GS-NS nanoparticles with the same LSPR peak (i.e., 900 nm), the extinction spectra of the GS-NS@SiO_2 nanoparticles exhibit the same maxima, as shown in Figure 5b. This result demonstrates that the silica shell has a minimal effect on the optical properties of the GS-NSs.

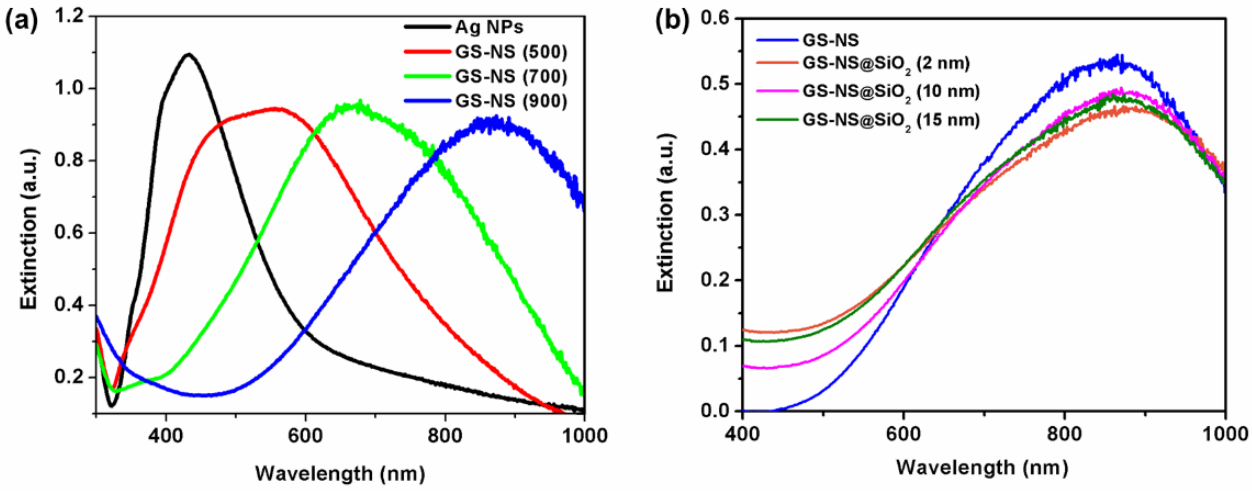

Figure 5. Extinction spectra of (a) AgNPs and GS-NSs with different maxima at 500 nm, 700 nm, and 900 nm (denoted as GS-NS (500), GS-NS (700), and GS-NS (900)), and (b) SiO_2-coated GS-NS with three different thicknesses of the silica shell.

SnO_2–Coated GS-NS Composites. Tin oxide is an attractive dielectric coating material for photocatalytic reactions due to its exceptional photostability and good carrier mobility. Yet, the latter characteristic can also lead to a slightly different role for the coating in our composite nanoparticle system. In lieu of the direct blocking of electron transfer, we anticipate that the SnO_2 shells will modulate charge transfer from the metal to the semiconductor and vice versa, which can further enhance the efficiency of the photocatalytic reactions occurring in the surrounding matrix. Additionally, we previously reported that tin oxide-coated gold nanoparticles are markedly more stable than silica-coated gold nanoparticles over a wide range of pH values.[6] This feature should lead to photocatalytic systems with enhanced stabilities and working lifetimes.

Therefore, we have explored the direct coating of tin oxide shells on GS-NSs to yield a core-shell structure (see Scheme 3). In our studies thus far, these nanoparticles have exhibited a broader optical activity in the NIR region compared to silica-coated nanoparticles; for the former, the corresponding extinction maxima range from 500 nm to 1000 nm. In addition, we have also explored the synthesis of GS-NSs coated with zinc- and antimony-doped tin oxide (Scheme 3). Related doped oxide tin films, which are commonly used as transparent conducting oxides (TCO), have the ability to modulate the band gap of tin oxide, which offers wide-ranging uses in photo-electrochemical reactions.[7-9] We have developed preliminary synthetic routes for generating these composite nanoparticles and evaluated their optical properties.

The various doped and un-doped tin oxide coated core-shell particles will also allow us to develop a better understanding of the fundamental mechanisms occurring within our composite ZIS photocatalytic system. We have sent these new nanoparticles to our collaborator, Prof. Tai-Chou Lee at National Central University in Taiwan, to evaluate their performance in hydrogen production via the photocatalyzed water-splitting reaction. Meanwhile, we have also developed an alternative recipe for synthesizing AgNPs that consistently yields particles having reproducible sizes and morphologies.

Scheme 3. Route Used to Prepare Gold-Silver Nanoshells (GS-NSs) coated with Tin Oxide, Antimony-Tin Oxide (ATO), and Zinc-Tin Oxide (ZTO).

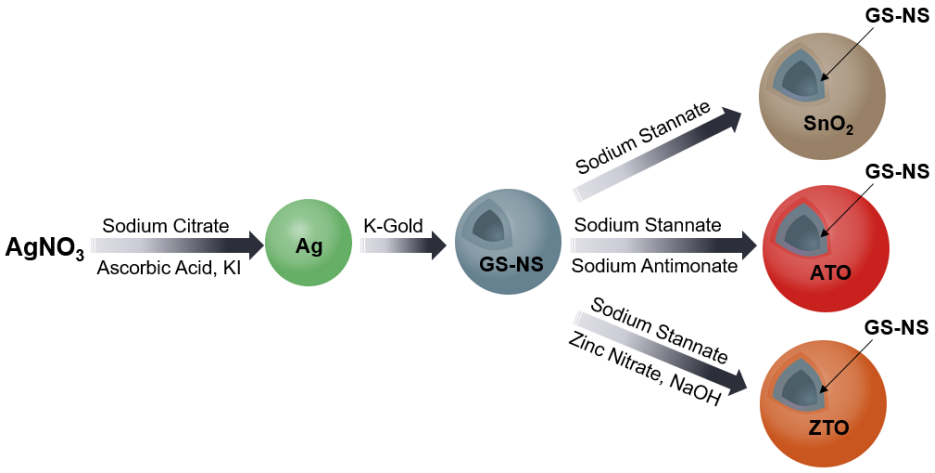

The TEM images shown in Figure 6 and the size measurements obtained using our Malvern Nanosight instrument (Figure 7) show the shell thicknesses on the GS-NS@ATO and GS-NS@ZTO samples are about 17 nm, while the bare SnO_2 shells are ~11 nm in thickness. We anticipate that this shell thickness will lead to an effective charge separation based on our previous time-resolved photoluminescence studies.[5]

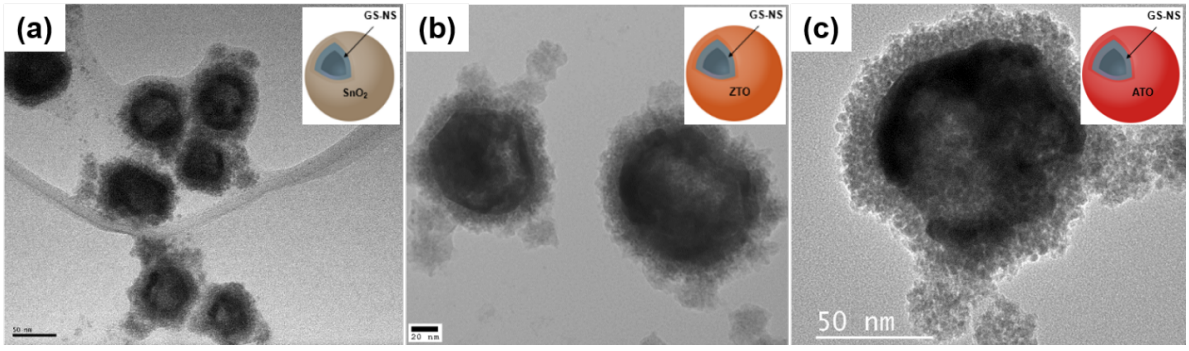

Figure 6. TEM images of (a) GS-NS@SnO_2, (b) GS-NS@ZTO, and (c) GS-NS@ATO NPs.

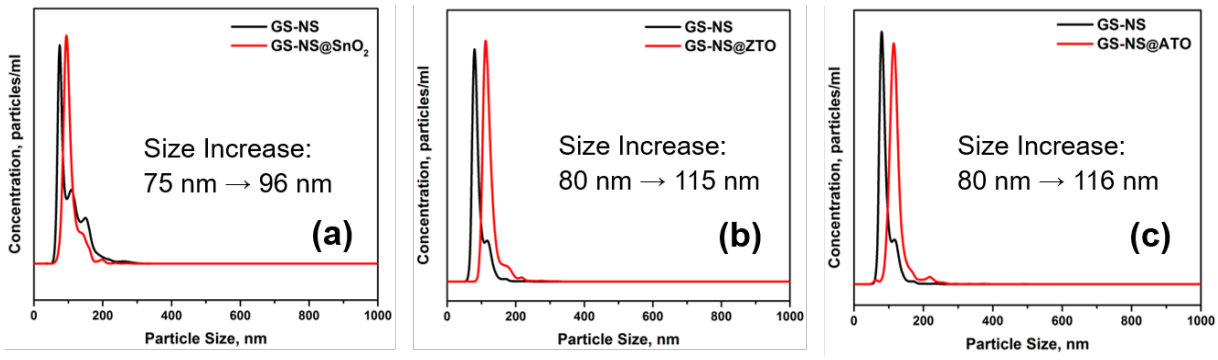

Figure 7. Malvern Nanosight size distribution plots for GS-NSs before and after coating with (a) SnO_2, (b) ZTO, and (c) ATO shells respectively.

Analysis of the optical properties of these nanoshells showed that the LSPR wavelength can be tuned using different amounts of the K-gold solution and by adjusting the reaction time in the galvanic replacement step, as shown in Figure 8.[5] The SnO_2 coating causes a red shift in the LSPR peak of the GS-NSs (by ~20-40 nm). This red shift is consistent with previous observations of coating the nanoparticles with a higher refractive index material, noting that the refractive index of SnO_2 (~2.006) is greater than that of water (~1.333).[10]

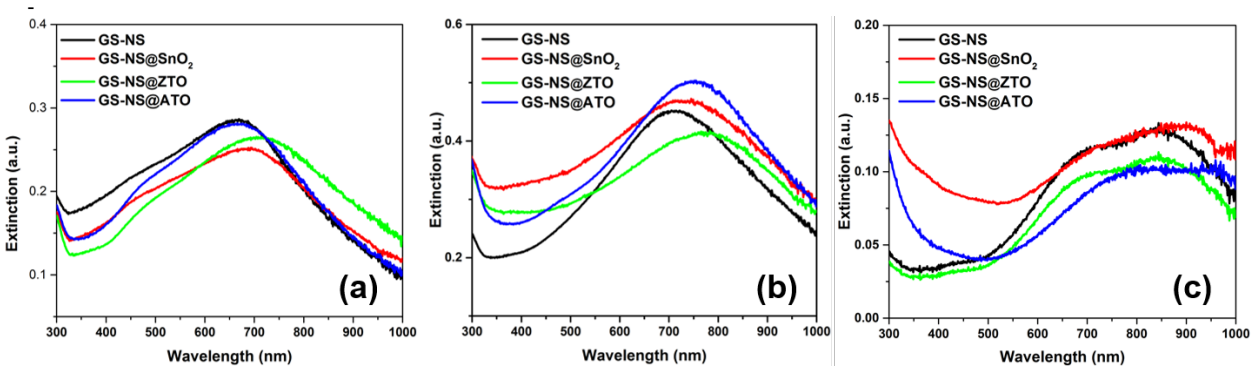

Figure 8. UV-Vis spectra of GS-NSs with different λ_{max} before and after coating with (a) SnO_2, (b) ZTO, and (c) ATO shells.

The ability to cast these SnO_2 coated nanoshells into a tin oxide thin film broadens their applicability as optically-responsive TCO films for solar, PEC, and photocatalytic applications.[11] We expanded our previously reported method of generating SnO_2 films embedded with AuNPs to embed GS-NS particles in SnO_2 thin films, since the latter nanoshells enjoy a wider extinction band in the visible region compared to bare AuNPs. Figure 9 shows the cross-sectional SEM image of a 250-nm thick SnO_2 thin film in which GS-NSs were embedded. We are currently exploring other promising thin-film materials and their corresponding electrical measurements.

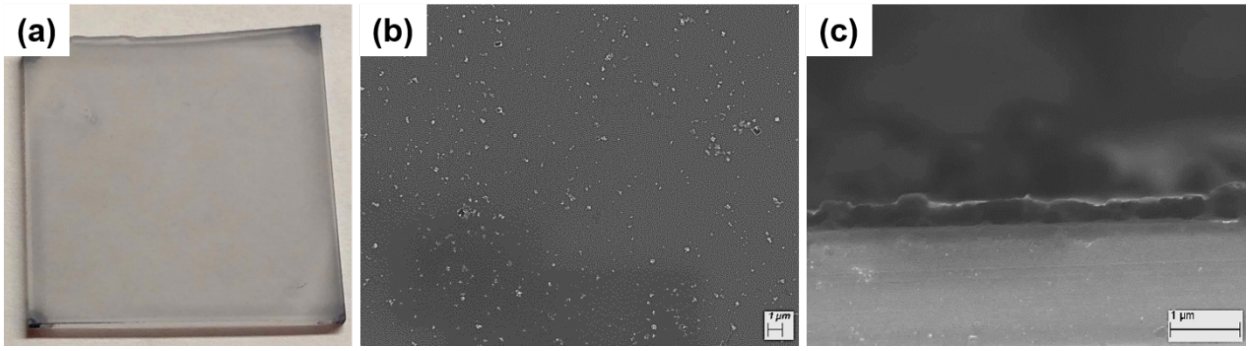

Figure 9. (a) Tin oxide thin film with embedded GS-NSs on a glass slide. (b) Top view and (c) cross-sectional view SEM images of GS-NSs embedded in tin oxide thin films on silicon wafer substrates.

3. Photonic iron oxide nanoparticles (Fe_3O_4) as co-catalysts in the water-splitting reaction

In separate studies, we explored the use of iron oxide (Fe_3O_4) nanoparticles as alternative co-catalysts for the water-splitting reaction. These photonic materials are inexpensive and exhibit similar extinction properties as noble metal nanoparticles. Furthermore, while many transitional metal oxides have shown excellent photocatalytic activity, they tend to absorb light in the UV region, which consists of only 5% of the total solar spectrum, thus giving rise to low photocatalytic efficiency.[12,13] However, Fe_3O_4 nanoparticles have a narrow band gap and are non-toxic semiconductors; moreover, they can be tuned to provide an alternative visible-NIR light-absorbing moiety in our composite photocatalytic system.

Using a modification of an established thermal decomposition method that purportedly affords highly crystalline NPs,[14] we recently prepared 30 nm Fe_3O_4 NPs. Figures 10a-c show the TEM, XRD, and UV-vis analysis of the resultant semi-crystalline nanospheres. We then designed an alternative thermal decomposition method that gave Fe_3O_4 NPs (Figure 10d) with greater crystallinity (see Figure 10e). We further evaluated the crystallinity of the two types of particles by calculating the crystallinity index (C.I.) based on the ratio of the average size measured by the TEM image and the average crystallite size calculated by the Debye-Scherrer equation. The C.I. of the Fe_3O_4 NPs synthesized using our new approach is ~1 versus ~2.8 for particles synthesized using the conventional method; notably, a C.I. value of 1 corresponds to a monocrystalline material. Comparing the extinction spectra of both types of Fe_3O_4 NPs, we note that NPs with a higher crystallinity exhibit a strong absorption band throughout the visible and NIR regions of the spectrum. The observed blue-shift in the extinction spectra of the less crystalline Fe_3O_4 NPs can be attributed to an increase in the band gap of the nanoparticles, due to their polycrystallinity, which leads to extinctions in the UV region. These studies and related studies of magnetic nanoparticles have led to three recent peer-reviewed publications.[15-17]

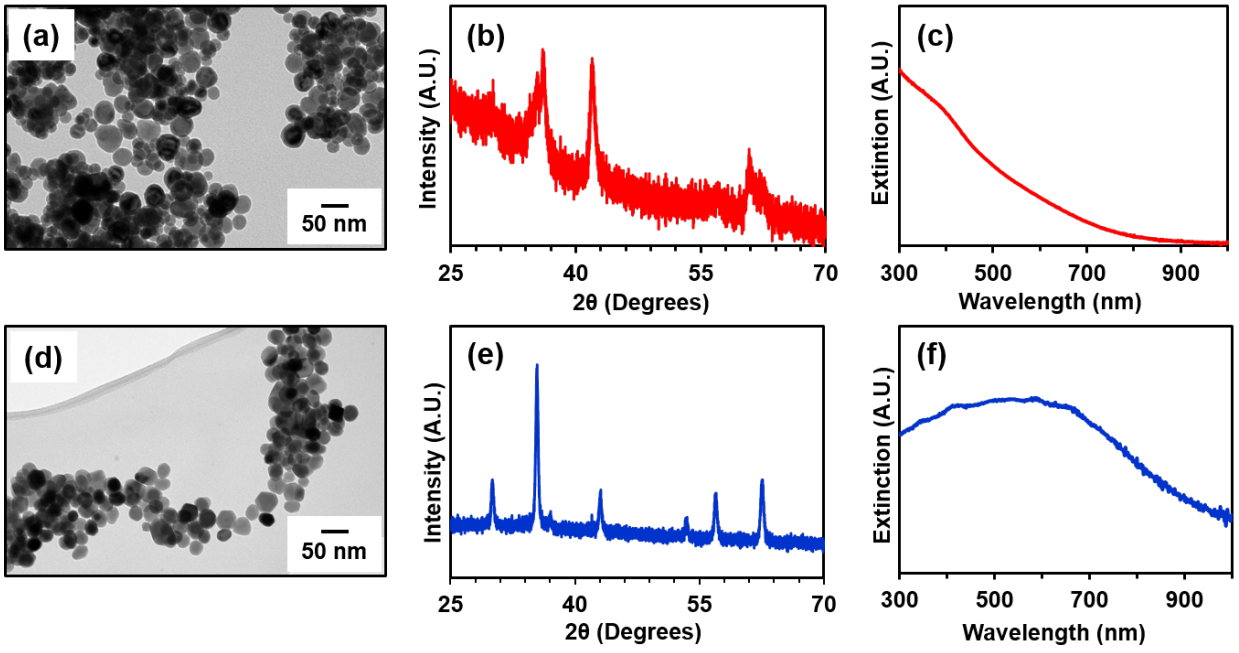

Figure 10. TEM images, XRD patterns, and extinction spectra of polycrystalline spherical Fe_3O_4 NPs (a-c) and monocrystalline Fe_3O_4 NPs (d-f).

List of Publications and Significant Collaborations

Publications

- Shakiba, A.; Zenasni, O.; Marquez, M. D.; Lee. T. R., Advanced Drug Delivery via Self-Assembled Monolayer-Coated Nanoparticles. *AIMS Bioengineering*, **2017**, *4*, 275-299. (AFOSR/AOARD FA2386-16-1-4067)
- Vittur, V.; Kolhatkar, A. G.; Shah, S.; Rusakova, I.; Litvinov, D.; Lee. T. R., Near-Infrared-Responsive, Superparamagnetic Au@Co Nanochains. *Beilstein J. Nanotechnol.,* **2017**, *8*, 1680-1687. (AFOSR/AOARD FA2386-16-1-4067)
- Chen, Y.-T; Kolhatkar, A. G.; Zenasni, O.; Xu, S.; Lee, T. R., Biosensing Using Magnetic Particle Detection Techniques. *Sensors*, **2017**, *17*, 2300. (AFOSR/AOARD FA2386-16-1-4067)
- Khantamat, O.; Li, C.-H.; Liu, S.-P.; Liu, T.; Lee, H.-J.; Zenasni, O.; Lee, T.-C.; Cai, C.; Lee. T. R., Tuning the Optical Properties of Anatase TiO_2 Nanospheres via Decoration with Partial Gold Shells for Broadening the Optical Response. *J. Coll. Interface Sci.*, **2017**, in revision. (DURIP FA9550-15-1-0374 and AFOSR/AOARD FA2386-16-1-4067)
- Kolhatkar, A. G.; Chen, Y.-T.; Chinwangso, P.; Nekrashevich, I.; Dannangoda, G. C.; Singh, A.; Jamison, A. C.; Zenasni, O.; Rusakova, I.; Martirosyan, K. S.; Litvinov, D.; Xu, S.; Willson, R. C.; Lee, T. R., The Magnetic Sensing Potential of Fe_3O_4 Nanocubes Exceeds that of Fe_3O_4 Nanospheres. *ACS Omega*, **2017**, in revision. (AFOSR/AOARD FA2386-16-1-4067)

Presentations

- T. R. Lee (2016, Oct.). Invited talk: National Central University; Taoyuan, Taiwan.
- T. R. Lee (2016, Oct). Invited talk: National Chiao Tung University; Hsinchu, Taiwan.
- T. R. Lee (2016, Nov). Invited talk: ACS Southwest Regional Meeting; Galveston, TX.
- P. Srinoi; T.R. Lee (2016, Nov). Poster: ACS Southwest Regional Meeting; Galveston, TX.
- R. Medhi; T.R. Lee (2016, Nov). Poster: ACS Southwest Regional Meeting; Galveston, TX.
- S. Shah; A. Shakiba; O. Zenasni; T.R. Lee (2016, Nov). Poster: ACS Southwest Regional Meeting; Galveston, TX.
- T. R. Lee (2017, Feb.). Invited talk: University of Iowa; Iowa City, IA.
- T. R. Lee (2017, Feb.). Invited talk: ACS on Campus; University of Houston; Houston, TX.
- T. R. Lee (2017, May). Plenary: ACS-Applied Materials & Interfaces Resource Chemistry Workshop; Shanghai Normal University; Shanghai, China.

Interaction/Collaboration with AFRL, DoD, Industry

- T. R. Lee (2016, Oct.). Met with representatives from Weatherford Corporation at the University of Houston to discuss research related to the AFOSR project.
- T. R. Lee (2017, May). Held discussions with Dr. Christopher Bunker (AFRL) regarding potential research collaborations.

Team Collaboration Synergy Highlights

- PI visit (2016, Oct), T. Randall Lee visited National Central University for one week.
- Student exchange (2017, Apr.), Mr. Yen-Chen Huang (from National Central University) visited the University of Houston for one month.

References

1. Khantamat, O.; Li, C.-H.; Yu, F.; Jamison, A. C.; Shih, W.-C.; Cai, C.; Lee, T. R. *ACS Appl. Mater. Interfaces* **2015**, *7*, 3981−3993.
2. Fagan, R.; McCormack, D. E.; Dionysiou, D. D.; Pillai, S. C. *Mater. Sci. Semicond. Process.* **2016**, *42, Part 1*, 2−14.
3. Wang, S.; Ding, Y.; Xu, S.; Zhang, Y.; Li, G.; Hu, L.; Dai, S. *Chem. Eur. J.* **2014**, *20*, 4916−4920.
4. Khantamat, O.; Li, C.-H.; Liu, S.-P.; Liu, T.; Lee, H. J.; Zenasni, O.; Lee, T.-C.; Cai, C.; Lee, T. R. *J. Colloid Interface Sci.*, in revision.
5. Li, C.-H.; Li, M.-C.; Liu, S.-P.; Jamison, A. C.; Lee, D.; Lee, T. R.; Lee, T.-C. *ACS Appl. Mater. Interfaces* **2016**, *8*, 9152−9161.
6. Lee, S. H.; Rusakova, I.; Hoffman, D. M.; Jacobson, A. J.; Lee, T. R. *ACS Appl. Mater. Interfaces* **2013**, *5*, 2479−2484.
7. Jain, G.; Kumar, R. *Opt. Mater.* **2004**, *26*, 27−31.
8. Babar, A. R.; Shinde, S. S.; Moholkar, A. V.; Bhosale, C. H.; Kim, J. H.; Rajpure, K. Y. *J. Semicond.* **2011**, *32*, 053001.
9. Bhat, J. S.; Maddani, K. I.; Karguppikar, A. M. *Bull. Mater. Sci.* **2006**, *29*, 331−337.
10. Oldfield, G.; Ung, T.; Mulvaney, P. *Adv. Mater.* **2000**, *12*, 1519−1522.
11. Lee, S. H.; Hoffman, D. M.; Jacobson, A. J.; Lee, T. R. *Chem. Mater.* **2013**, *25*, 4697−4702.
12. Chen, H.; Wang, L. *Beilstein J. Nanotechnol.* **2014**, *5*, 696−710.
13. Ola, O.; Maroto-Valer, M. M. *J. Photochem. Photobiol. C,* **2015**, *24*, 16−42.
14. Chen, H.; Burnett, J.; Zhang, F.; Zhang, J.; Paholak, H.; Sun, D. *J. Mater. Chem. B* **2014**, *2*, 757−765.
15. Vittur, V.; Kolhatkar, A. G.; Shah, S.; Rusakova, I.; Litvinov, D.; Lee. T. R., Near-Infrared-Responsive, Superparamagnetic Au@Co Nanochains. *Beilstein J. Nanotechnol.,* **2017**, *8*, 1680-1687.
16. Chen, Y.-T; Kolhatkar, A. G.; Zenasni, O.; Xu, S.; Lee, T. R., Biosensing Using Magnetic Particle Detection Techniques. *Sensors*, **2017**, *17*, 2300.
17. Kolhatkar, A. G.; Chen, Y.-T.; Chinwangso, P.; Nekrashevich, I.; Dannangoda, G. C.; Singh, A.; Jamison, A. C.; Zenasni, O.; Rusakova, I.; Martirosyan, K. S.; Litvinov, D.; Xu, S.; Willson, R. C.; Lee, T. R., The Magnetic Sensing Potential of Fe_3O_4 Nanocubes Exceeds that of Fe_3O_4 Nanospheres. *ACS Omega*, **2017**, in revision.